CHEMISTRY
A EUROPEAN JOURNAL

FULL PAPER

DOI: 10.1002/chem.200((will be filled in by the editorial staff))

In Silico Designed Novel Mechanoresponsive Materials

G. Prampolini[a],*, F. Bellina[b], M. Biczysko[c], C. Cappelli[b,d], L. Carta[d], M. Lessi[b], A. Pucci[b,e], G. Ruggeri[a,b] , V. Barone[d]

Abstract: The possibility of exploiting supramolecular architectures to design and synthesize novel soft smart materials with specific optical and mechanical properties has recently attracted a lot of attention, in view of the various technological applications in material engineering. Due to the multiplicity of all possible combinations of building blocks, which concur both to the supramolecular aggregate formation and to the tuning of the wanted functionalities, the design of these materials can greatly benefit, in terms of costs and time, from an *in silico* screening approach. Following this idea, the optical properties of a novel, not yet synthesized, family of organic chromophores is first investigated through state-of-the-art quantum mechanical calculations, to spot those homologues which exhibit the best spectral features, in terms of absorption/emission relative position and intensity, Stokes shift, etc. The best candidates are then effectively synthesized, and their predicted optical behavior verified through the comparison of measured and computed absorption and emission spectra. The resulting good agreement, prompted us to introduce one of the targeted compounds into a polyethylene matrix by dispersion, indeed achieving an " *in silico* designed" mechanochromic material. Besides this novel material can find application itself, the integration of computational and experimental techniques here reported defines an efficient protocol that can be applied to make a selection among very similar dye candidates, which constitute the essential responsive part of such supramolecular devices.

Keywords: computational spectroscopy • mechanochromic materials • in silico design • vibronic models

[a] Dr. G. Prampolini
Istituto per i Processi Chimico Fisici
Consiglio Nazionale per le Ricerche
Area della Ricerca, via Moruzzi 1, I-56125 Pisa, Italy
Fax: +39-050-3152230
E-mail: giacomo.prampolini@pi.ipcf.cnr.it

[b] Prof. F. Bellina, Dr. C. Cappelli, Dr. M. Lessi, Dr. A. Pucci and Prof. G. Ruggeri
Dipartimento di Chimica e Chimica Industriale
Università di Pisa
via Risorgimento 35, I-56126 Pisa, Italy

[c] Dr. M. Biczysko
Center for Nanotechnology Innovation@NEST
Istituto Italiano di Tecnologia
Piazza San Silvestro 12, I-56127 Pisa, Italy

[d] L. Carta, Dr. C. Cappelli and Prof. V. Barone
Classe di Scienze
Scuola Normale Superiore
Piazza dei Cavalieri 7, I-56126 Pisa, Italy

[e] Dr. A. Pucci
CNR NANO
Istituto Nanoscienze-CNR
Piazza San Silvestro 12, I-56127 Pisa, Italy

Supporting information for this article is available on the WWW under

Introduction

Impressive progress in material engineering and in the design of nanohybrid compounds has been inspired in the past few decades by the growing interest in new soft "smart" materials, endowed with unique optical properties that can be tuned and controlled by external stimuli (light, heat, mechanical stress, pH variations etc.).[1] "Smart" devices can thus be designed for many different applications, among which camouflage systems, anti-counterfeiting, attoreactor sensors, informational displays or white emitting vesicles. Soft intelligent materials, including among others synthetic polymers, are based on the assembly of different units performing specific functions; for example, compounds able to respond to a wide variety of stimuli can be inserted within polymeric matrices (either in interfacial regions or in more complex supramolecular architectures) to obtain highly tuneable platforms.[2] Among these mechanoresponsive materials, thanks to their possible use for efficient *in situ* sensing, particular attention has been recently[3]

devoted to that class of compounds, referred to as mechanochromic, whose color (in absorption and/or fluorescence) changes upon mechanical stress. In this case, since commercial processable polymeric matrices (polymer commodities) display negligible electronic response in the technologically relevant frequency range (from visible to near-infrared), color and photoresponse are most conveniently achieved by introducing properly designed active species in the polymeric matrix.[4] Organic chromophores, usually based on extended π-conjugated structures, show large photoresponses in a spectral region that can be easily tuned from the visible to the near-infrared by appropriate molecular design. The possible formation of supramolecular dye architectures adds one more layer of complexity to the problem, opening at the same time a wealth of exciting opportunities. With respect to the isolated chromophores, molecular aggregates can display entirely new features, and are extremely sensitive to medium properties, so that aggregachromic materials have been developed exploiting precisely this sensitivity.[3, 5] In any case, the crucial and responsive part of a mechanochromic material is the organic chromophore, either chemically linked onto the polymeric support or blended into it. In the latter case some general criteria that should be satisfied by the dye can be defined,[3b] as a rigid rod-like shape or the presence of electron withdrawing or donating groups on the dye's aromatic core. However, the choice of the best candidate, among a set of similar target chromophores, may result rather difficult, since an accurate prediction of the spectral features (including Stokes shift or line shapes) can become very cumbersome if solely based on chemical intuition.

In this framework, the availability of reliable and predictive computational methods[2, 6] can be very beneficial, since the results of a *in silico* screening can effectively guide the synthetic work, with obvious benefits in terms of costs and time. Clearly, a strong interplay between theoreticians and experimentalists is required. For instance, when dealing with mechanochromic materials, it is crucial to select those chromophoric units that have some of the following characteristics: a well oriented transition dipole, a large Stokes shift for high emission efficiency, optical behavior depending on the aggregation extent and, in case of anti-counterfeiting needs, strong absorption in the near UV region and emission in the visible range.[3b] In particular, once a basic molecular candidate possessing the required features has been spotted by the experiment, an *in silico* screening can be performed on a larger set of homologues, differing from the parent chromophore by a small number of substituent groups. Once one or more targets are identified by calculations, the experimental efforts may be concentrated on them. Such a conceptual procedure can be successful only if the computational predictions are reliable, and appropriate approaches are therefore required, allowing the direct simulation of spectroscopic signals, while retaining a reasonable computational cost. This request appears to be satisfied by DFT based methods, whose reliability in simulating the spectral properties of molecular organic systems of medium up to large dimensions has been widely reported.[7] Moreover, recent extensions have demonstrated that not only vertical absorption and emission transitions can be reliably obtained, but that also spectral shapes can be directly simulated.[8] In the design protocol here presented, computational methods will be first employed in the *in silico* screening of UV-Vis absorption and emission energies for a series of not yet synthesized and potentially interesting chromophores, based on the same aromatic skeleton and bearing substituent groups of different nature in terms of electron-donating and electron-accepting capability. Once the best compound is identified according to the requisite features, it is effectively synthesized and characterized by measuring its absorption and emission spectra in solution. The obtained experimental spectra will be compared with the computed ones, to assess the quality of the predictions. Eventually, the target chromophore is dispersed in a linear low-density polyethylene (LLDPE) matrix, and optical properties of the final mechanochromic material are investigated. In particular, we will focus on novel thienyl-substituted 1,4-bis-ethynylbenzenes **1** bearing donor and acceptor groups on the two terminal thiophene rings (Figure 1). Indeed, this class of dyes is characterized by a rod-like highly conjugated molecular structure, which also results easily functionalizable by push-pull peripheral groups.

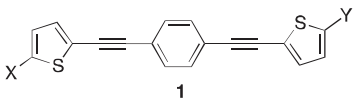

1

Figure 1. General structure of thienyl-substituted 1,4-bis-ethynylbenzenes **1**

Moreover, the high electron delocalization of such compounds, favored by the presence of the central benzene and the two lateral conjugated thiophene rings, should in principle give rise to bright absorption/emission in the UV/visible range, and on the other hand be very sensitive to the nature of the push/pull substituents, still under the hypothesis that different push/pull pairs could be able to sensitively shift the absorption/emission maximum wavelength towards different spectral regions.

Results and Discussion

1. **Validation of the protocol**

1.1 *Computational methodology*. The most popular, Vertical Energy (VE) approach for the calculation of electronic spectra (UV–Vis, Circular Dichroism, photoelectron, X-ray, *etc.*) still relies on the computation of vertical excitation energies, which are further convoluted to simulate line-shapes. Such a treatment completely neglects the influence of nuclear motions, despite the well-recognized notion that a proper account of vibrational effects is often mandatory in order to interpret correctly the experimental findings.[7] In this respect, the calculation of reliable linear electronic spectra, including vibronic contributions (Vertical Gradient (VG), Adiabatic Shift (AS) or Adiabatic Hessian (AH) approaches, see Supporting information for details), has recently become feasible for medium-to-large systems,[8-9] and in several cases the inclusion of vibrational contributions is a key factor for a correct interpretation of the experimental outcomes.[6j, 10] Moreover, the predicted data can also depend upon the complexity of the environment, a solvent or a polymeric matrix, actually interacting with the chromophore. To a first approximation, the surrounding environment can be taken into account in a time-independent approach by employing continuum solvation models,[6e, 6f, 11] which provide rather accurate results at a relatively low computational cost and can be extended to several spectroscopic properties,[6c, 12] with the further consideration of spectral line shapes.[12c, 13] A first assessment of the adequacy of the chosen computational model, *i.e.* choice of the DFT functional/basis set, VG and AS approximations and solvation model, has been performed on a p-diethinylbenzene derivative, by comparing the computed spectra with their

experimental counterpart.[14] All details of this first validation can be found in the Supporting Information.

In order to confirm the transferability of the adopted computational models to the class of target molecules considered in the present work, prior to the analysis of simulated VG and AS spectra, all different theoretical models were also validated for the lowest electronic transition of a reference compound. This has been identified in the simplest homologue of the series, 1,4-bis(thiophen-2-ylethynyl)benzene (**1a)** (X = Y = H, Figure 1).

As far as adiabatic approaches are concerned, the spectra simulated within AS and AH models are presented in Figure 2, allowing us to discuss the possible influence of frequency changes and normal mode rotation between initial and final states. Both spectra show very similar line-shapes, but slightly shifted positions, namely about 10 nm for both absorption and emission. More important, the abovementioned shift has the same sign for absorption and emission (being in both cases the AS maximum wavelength less than the one computed with the AH approximation), so that the predicted Stokes shift remains almost unaltered. These results suggest that Duschinsky effects do not play significant role and in this case can be safely neglected by adopting the less expensive AS approximation. Next, before comparing the vertical and adiabatic models, it should be noted that the difference between VG and AS is solely related to the approximation used to estimate the shift between the normal modes of the two involved electronic states: while in adiabatic methods the true shift is computed, an 'effective' shift is used in the vertical approach. When the harmonic approximation is exact, the vertical and adiabatic approaches are equivalent, and in the present case the good agreement between VG and AS spectra confirms the reliability of such an approach. It may be worth noticing that the difference between AH and VG is again related mainly to frequency changes. These lead to the shift of the <0|0> transition (in analogy to the AS model) and to slightly different relative positions of vibronic absorption maxima. However, both spectra show very similar overall line-shapes.

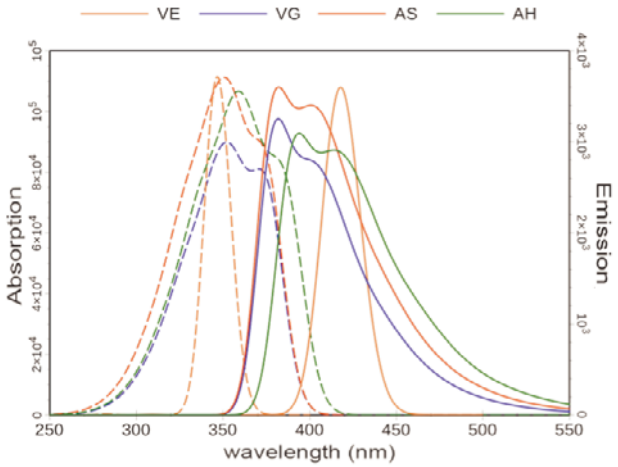

Figure 2. Absorption (dashed lines) and emission (solid lines) spectra, computed on reference compound 1a using different theoretical models: Vertical Energy (VE, orange lines), Vertical Gradient (VG, blue lines), Adiabatic shift (AS, red lines) and Adiabatic Hessian (AH, green lines). All spectra are convoluted with a Gaussian function of 750 cm^{-1} of half width at half maximum (HWHM). Absorption intensity: molar absorption coefficient in $dm^3\ mol^{-1}\ cm^{-1}$, emission intensity in $\mu J\ mol^{-1}\ s^{-1}$.

On these grounds, application of both VG and AS models to simulate broad spectral features of chromophores considered in this work is fully validated. We only note that adiabatic approaches should be always considered for a detailed analysis of well-resolved experimental spectra. Finally, in Figure 2 are also reported the absorption/emission peaks resulting from the application of the low level vertical excitation (VE) model. It appears that, besides the loss of information concerning the band shape, the maximum absorption wavelength is well reproduced with respect to higher-level techniques, whereas a larger error is found for the emission. Moreover, since absorption and emission VE errors have opposite sign, an overestimation of the Stokes shift is to be expected in this case.

1.2 *Screening capabilities*. The reliability of the screening procedure has been further validated by performing calculations on bis-ethynyl benzenes (**1b-e)**. All these homologues present the same central unit, to which substituents of different nature in terms of acceptor/donor capability are linked. After the simulation of their absorption and emission spectra, compounds **1b-d** were prepared according to a two-step reaction sequence involving: a) a Cassar-Heck reaction between the trimethylsilyl-protected □-bridge **3** and a 5-substituted 2-bromothiophene **4**, and b) a novel Pd/Cu catalyzed Sila-Sonogashira cross-coupling between the trimethylsilyl-protected alkynes **5**, resulting from step (a), and bromides **4** (Scheme 1). In details, when ((4-ethynylphenyl)ethynyl)trimethylsilane (**3**)[15] was reacted with bromides **4a-b** in the presence of 5 mol% $PdCl_2(PhCN)_2$, 10 mol% *t*-Bu_3P, 2.0 equiv DABCO as the base in MeCN at room temperature,[16] the required alkynes **5a-b** were isolated in 60 and 65% yield, respectively (Scheme 1). The target chromophores **1b-d** were successfully obtained from the Sila-Sonogashira type coupling under PTC conditions, according to a recent synthetic protocol developed by us,[17] involving trimethylsilylalkynes **5a-b** and thienyl bromides **4b-d**. In this way, thiophene-based derivatives **1b-d** were isolated in 50-95 % yields. Similarly, the symmetrically-substituted derivative **1e** was obtained with 68% isolated yield by reacting a molar excess of bromide **4a** with 1,4-bis((trimethylsilyl)ethynyl)benzene (**6**) (Scheme 2).

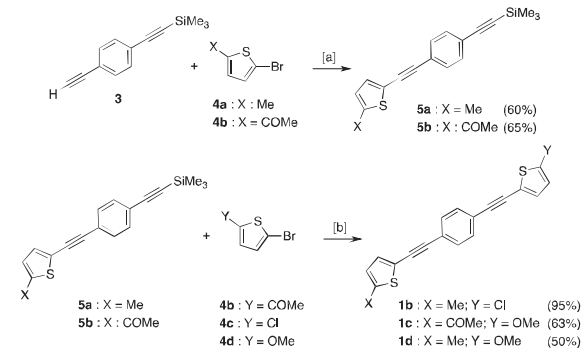

[a] : $PdCl_2(PhCN)_2$ (5 mol%), *t*-Bu_3P (10 mol%), DABCO (2.0 equiv), MeCN (1M), room temperature, 5-18h.
[b] : $PdCl_2(PhCN)_2$ (5 mol%), *t*-Bu_3PHBF_4 (10 mol%), CuI (10 mol%), $BnBu_3NCl$ (20 mol%), toluene, $NaOH_{aq}$, 40 °C, 18h.

Scheme 1. Synthesis of compounds 1b-d.

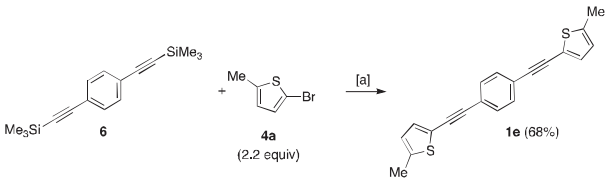

[a] : $PdCl_2(PhCN)_2$ (5 mol%), t-Bu_3PHBF_4 (10 mol%), CuI (10 mol%), $BnBu_3NCl$ (20 mol%), toluene, $NaOH_{aq}$, 40 °C, 18h.

Scheme 2. Synthesis of compound 1e.

The absorption and emission spectra of **1b-e** were experimentally measured in THF solution, *i.e.* with the same solvent employed in calculations. Results are listed in Table 1 and compared to calculated VE, VG and AS excitation or emission energies. The whole computed spectra are reported in Figure 3.

Table 1. Computed and experimental maximum absorption/emission wavelengths (λ^{max}) of compounds 1b-e.

	Absorption (λ^{max}, nm)				Emission (λ^{max}, nm)			
	VE	VG	AS	Exp	VE	VG	AS	Exp
1b	354	350	350	348	427	392	395	400
1c	376	374	373	368	462	420	424	bb[a]
1d	359	362	364	352	433	395	398	bb[b]
1e	353	350	349	348	426	392	395	395

[a] Broad band (bb) from 420 to 570 nm. [b] Broad band from 395 to 460 nm

The VE approach is able to well reproduce absorption maxima, with an average error between calculated and experimental values of about 6 nm. Even more relevant is the fact that the calculations are able to correctly reproduce the experimental trend moving from one chromophore to the other (*i.e.* **1b** ≈ **1e** < **1b** < **1c**). In addition, in all cases the most intense transition is due to a HOMO – LUMO excitation, involving the frontier orbitals of π-character, so that the electronic transition of interest can be classified as π→π*. Moving to emission, as already found for the reference **1a** compound, the VE approach gives less accurate results and is therefore less effective for reliable predictions. For instance, in compounds **1b** and **1e**, a larger average error between experiments and calculations is obtained (around 20 nm). Furthermore, the absence in the VE approach of any reliable treatment of the line-shape makes difficult the comparison and assignment of the experimental and calculated absorption maxima. This is most evident for the emission band of compounds **1c** and **1d**, where the broad shape of the experimental band makes a precise assignment of the maximum emission wavelength rather questionable. For such reasons, a simple check on vertical excitation energies has been followed by more refined VG and AS approaches.

Inspection of Figure 3 confirms the ability of both VG and AS approaches to give a maximum absorption wavelength in excellent agreement with experiment, but also to accurately describe the experimental line-shapes. More important, the improvement with respect to VE is most significant for emission than for absorption. In fact, the increased accuracy of the vibronic approaches is apparent for the **1b** and **1e** chromophores, for which the separation between the two most intense peaks is now evident and very well

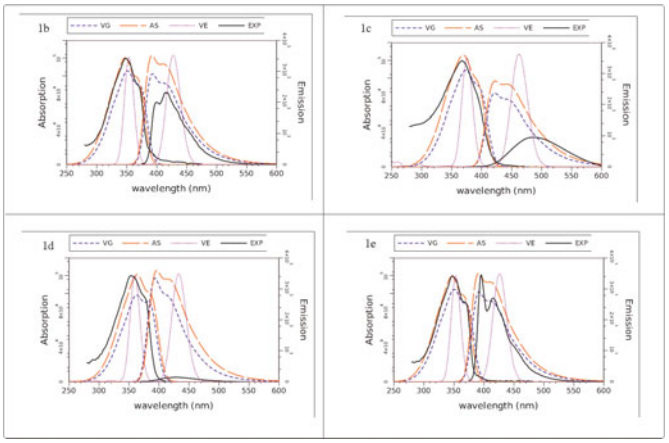

Figure 3. Computed and experimental spectra are shown for compound 1a to 1d. Experimental spectra are reported with a black solid line. Blue (dashed), red (solid) and magenta (dotted) lines are employed for spectra computed in the VE, VG and AS approximations, respectively. Absorption intensity: molar absorption coefficient in dm^3 mol^{-1} cm^{-1}, emission intensity in μJ mol^{-1} s^{-1}.

Table 2. VE screening results: predicted maximum absorption/emission wavelengths and Stokes shifts

X	Y	Absorption (nm)	Emission (nm)	Stokes shift (nm)
H	H	347	418	71
	CHO	377	463	86
	$CH=(C_9H_4O_2)$	434	534	100
OH	$CH=C(CN)_2$	426	527	101
	CH=C(CN)(COOH)	418	520	102
	COOH	370	454	84
	CHO	370	461	91
	$CH=(C_9H_4O_2)$	433	529	96
SH	$CH=C(CN)_2$	419	520	101
	CH=C(CN)(COOH)	412	516	104
	COOH	364	454	90
	CHO	388	491	103
	$CH=(C_9H_4O_2)$	442	562	120
NH_2	$CH=C(CN)_2$	436	567	131
	CH=C(CN)(COOH)	428	558	130
	COOH	382	479	97

reproduced, and the accuracy of the predicted maximum wavelength peak is increased, with respect to VE computed values, by roughly a factor of 2. As already noted, the emission bands obtained experimentally for compounds **1c** and **1d** are rather broad and do not present any clear pattern of vibrational structure. This makes the comparison with their simulated counterparts rather difficult. Broadly speaking, as far as **1d** is concerned, VG and AS (but also VE) spectra fall within the wide spectral region (395 – 460 nm) interested by the experimental emission. On the contrary, despite being more intense with respect to the former, the experimental emission band registered for compound **1c** seems more red shifted with respect to the values computed at all levels, although an overlap with the VG and AS line-shapes in the lowest energy regions is still present.

2. **Screening**

Based on the previous results, in particular on the capability of the VE approach to preserve the correct ordering of the maximum absorption wavelengths, the screening of the absorption properties of the selected target set of homologues was performed at this level. Indeed, notwithstanding the better quality of the VG and/or AS predictions, computational convenience has prompted us to employ the simple and cheap VE technique. Similarly, although the computational cost of emission VG/AS spectra is certainly balanced by the gain in accuracy and reliability, the large dimensions of the target set suggested us to perform the preliminary screening on emission still at the VE level. Based on VE screening results, a restricted set of homologues will be selected and thereafter considered for AS calculations. The final target compound to be effectively synthesized will be thus chosen within this second restricted set.

The VE screening results are reported in Table 2, by specifying, for each homologue of the target set, the position of the absorption and emission peaks and the computed Stokes shifts. It appears that different pairs of X and Y substituents (see Figure 1) highly influence the absorption/emission peak positions. The **1a** homologue is reported in the first row and can be taken as reference to evaluate the direction of the computed shifts. In this respect, all X/Y pairs shift toward larger values, *i.e.* lower energy regions of the spectrum, both in absorption and in emission. In the former case, as far as 'pull' substituents are concerned, the maximum shift (around 90 nm with respect to **1a**) is observed with Y= (CH=($C_9H_4O_2$)), while the minimum one (about 30 nm) is registered when aldehydic or carboxylic groups are employed. Also the red shifts due to the X 'push' substitutions appear, for a given Y, rather regular, with NH_2 > OH ≈ SH. The predicted red shift in emission with respect to **1a** is even more marked, being as large as 100 nm. In other words, the substitution of hydrogen atoms with the selected X/Y pairs systematically increases the Stokes shift. It may be worth noticing that, at variance with absorption, no regular trend can be spotted on Y substitution for a given X. For instance, the red shift caused by the CH=($C_9H_4O_2$) and CH=$C(CN)_2$ Y substituents, amounts to 111 and 102 nm, respectively when combined with X = SH, and 144 and 149 nm when combined with X = NH_2. These results indicate the absence of a clear trend and rule out the possibility of a simple rationalization of the results, based only on 'push/pull' effects, highlighting the important role that an *in silico* screening can play in the molecular design. Moreover, it can be speculated that additional important information can be obtained from more sophisticated pre-screening procedures, not limited to computation of vertical energies and transition strengths, but allowing for a direct simulation of experimental outcomes.

Based on the former VE screening, a new restricted screening set has been extracted, considering that the largest Stokes shift is registered for chromophores substituted with Y=CH=$C(CN)_2$. Absorption and emission spectra have been therefore simulated at AS level for this "pull" group in combination with all three considered "push" ones, giving rise to target compounds **1f**, **1g** and **1h** (X = OH, SH and NH_2, respectively; Figure 4).

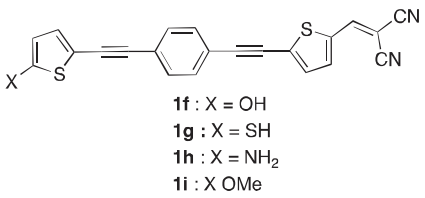

1f : X = OH
1g : X = SH
1h : X = NH_2
1i : X OMe

Figure 4. Chemical structures of compounds 1f-i

Indeed, the computed spectra, presented in Figure 5, clearly show that the final target cannot be identified among the considered homologues solely based on VE results. In fact, despite **1h** seems to be the most promising target (Table 2), due to the largest Stoke Shift computed at this level and the similar transition intensities found for all three compounds, direct simulation of absorption and emission spectra evidences (Figure 5), that although **1h** shows the largest spectral window between absorption and emission maxima, at the same time much lower absorption and, even more important, emission intensities are to be expected.

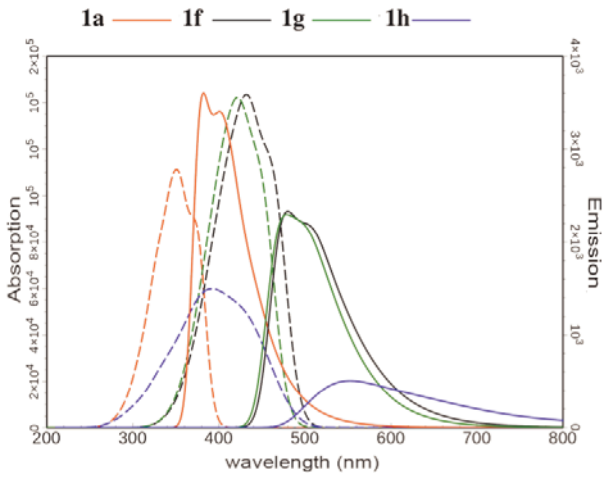

Figure 5. Absorption (dashed line) and emission (solid lines) spectra of the restricted screening set, reported along with the reference 1a compound. All spectra have been simulated within AS approach and convoluted with a Gaussian function of 750 cm^{-1} HWHM. Absorption intensity: molar absorption coefficient in dm^3 mol^{-1} cm^{-1}, emission intensity in μJ mol^{-1} s^{-1}.

For such reasons the **1f** and **1g** chromophores, showing large Stoke Shift and at the same time good absorption and emission features are more suitable for the applications here considered. Between the latter two systems, **1g** (*i.e.* the one with X=SH) may show some disadvantages related to the significant change of the steric position of SH group upon electronic excitation. Therefore, **1f** has been suggested as the best candidate for further development. However, because we had to take into account the necessity of modulating the interaction between the dye molecule and its miscibility within a polymer matrix, compound **1i** (in which the

hydroxyl "push" substituent was replaced by a methoxyl group) was finally chosen as the target chromophore to be prepared.

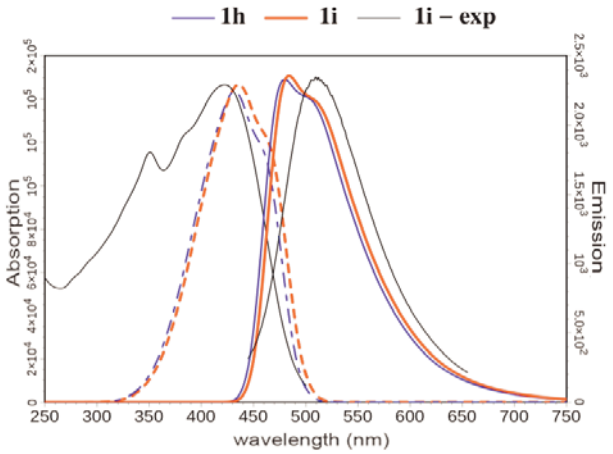

Figure 6. Experimental (black solid lines) and computed (blue dashed and solid lines for absorption and emission, respectively) spectra of the final target compound 1i. Computed spectra for 1f are reported with blue lines for comparison. All spectra simulated within the AS approach and convoluted with a Gaussian function of 750 cm^{-1} HWHM. Absorption intensity: in dm^3 mol^{-1} cm^{-1}, emission intensity in µJ mol^{-1} s^{-1}.

Absorption and emission bands were re-computed according to this latter substitution: the resulting spectra are reported in Figure 6, together with the ones obtained for the homologue **1f**. It is worth mentioning that in this case, both absorption and emission spectra were computed at the AS level, to enforce the prediction and improve the comparison with the experimental band.

3. **Synthesis and experimental characterization of compound 1i.**
Compound **1i** was synthesized according to the reaction sequence summarized in Scheme 3, and its absorption/emission spectra recorded in a THF solution.

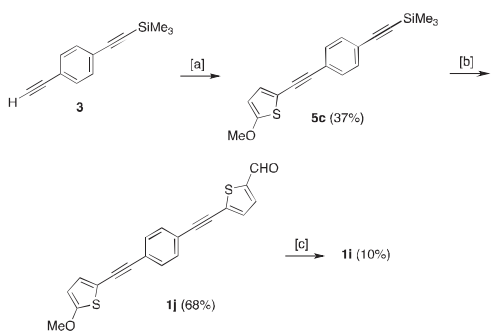

[a] : 2-bromo-5-methoxythiophene (**4d**) (0.9 equiv), $PdCl_2(PhCN)_2$ (5 mol%), t-Bu_3P (10 mol%), DABCO (2.0 equiv), MeCN (1M), 18h, RT. [b] : 5-bromothiophene-2-carbaldehyde (**4e**) (0.9 equiv), $PdCl_2(PhCN)_2$ (5 mol%), t-Bu_3PHBF_4 (10 mol%), CuI (10 mol%), $BnBu_3NCl$ (20 mol%), toluene, $NaOH_{aq}$, 40 °C, 16h. [c]: $NC(CH_2)CN$ (1.2 equiv), piperidine (cat), EtOH, 80 °C, 2.5h.

Scheme 3. Synthesis of compound **1i**.

The resulting peaks were found at 422 nm in absorption and at 512 nm in emission. The *a posteriori* experimental spectra are also reported in Fig. 6. The agreement with the theoretical predictions is very good, both for absorption and emission peaks and intensities. Moreover, use of the AS method allowed us to predict a line-shape which is also in good agreement with the experimental bands.

Finally, in line with the validation results, the overall reproduction of the absorption spectrum is better than the one found for emission, resulting in a slightly underestimated Stokes shift. However, all in all, the computed screening succeeded in indicating a target chromophore with the chosen characteristics.

4. **Dispersion into polymeric matrix and properties of the 'designed' compound.**

Once the predicted spectroscopic behavior of target chromophore **1i** was confirmed, this dye was coupled with a polymeric matrix to assemble the smart material, final aim of this work. First, 0.02 wt% of **1i** dispersed within a LLDPE matrix showed absorption bands at 450 and 480 nm, respectively, about 25 nm red-shifted with respect to THF solution. Conversely, the emission of the film was pointed at 498 nm, that is 14 nm blue-shifted compared with **1i** in solution (Figure 7).

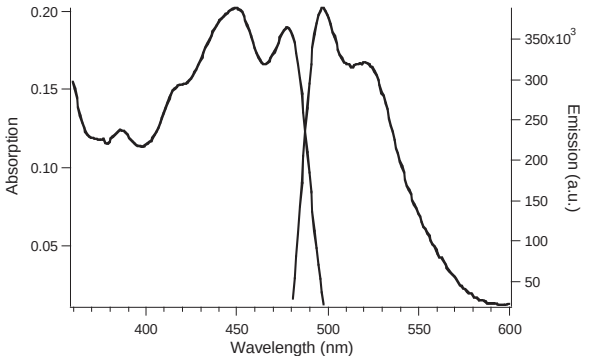

Figure 7. UV-Vis absorption (left) and emission (right) spectra of a LLDPE film containing the 0.02 wt% of **1i**.

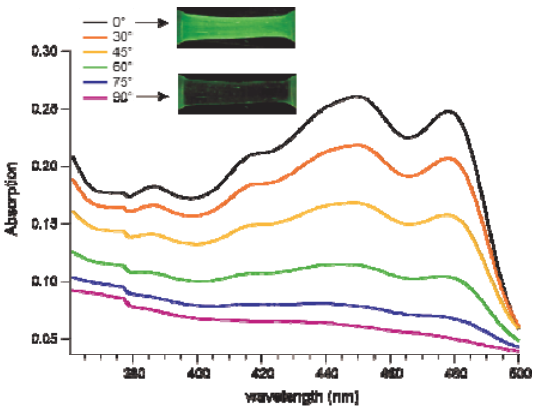

Figure 8 UV-Vis absorption spectra as a function of the polarization angle θ of a LLDPE oriented film (Dr = 5) containing the 0.02 wt% of 1i. Inset: digital images of the film under near-UV light (366 nm), observed through a linear polarizer

Moreover, the overall vibronic pattern of the optical bands is also different, possibly due to increased rigidity provided by the polymeric environment. These characteristics can be also attributed to the poor molecular interaction between **1i** chromophores and the aliphatic repeating units of the supporting LLDPE matrix, even though no spectral bands attributed to the formation of dye aggregates are found at this concentration. The high dispersion degree of **1i** within LLDPE was confirmed by UV-Vis experiments in linearly polarized light (Figure 8) carried out on the uniaxially oriented film (drawing ratio Dr = 5). When the polarization of the

incident light is parallel to the stretching direction (= 0°), the film showed a absorption maximum pointed at 450 nm. On the contrary, in the perpendicular configuration (= 90°) the absorption band results mostly suppressed, thus clearly indicating a pronounced anisotropic behavior. The dichroic ratio R is as high as 25 thanks both to its rod-like shape, which allows the transition dipole moment to be well aligned to the molecular axis,[18] and to its dispersion within PE at a molecular level. The same behavior was recorded in emission as evidenced by images of the film taken under the illumination of a 366 nm UV lamp with the superimposition of a linear polarizer oriented parallel and perpendicular to the drawing direction (Figure 8, inset).

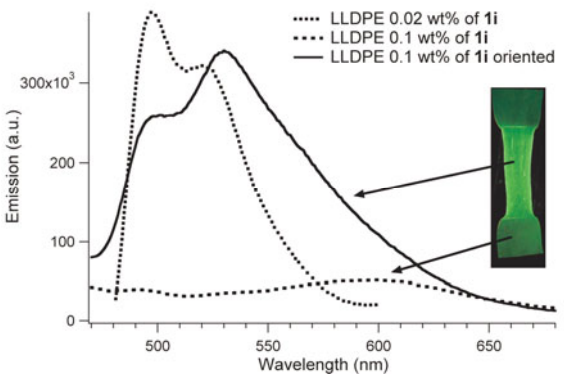

Figure 9. Emission of a LLDPE film containing the 0.02 and the 0.1 wt% of 1i before and after orientation at Dr = 5. Inset: digital image of the oriented film under irradiation at 366 nm.

As analogously reported in literature for perylene-based dyes[19], by increasing **1i** concentration within LLDPE (from 0.02 to 0.1 wt%) the fluorescence of the film resulted mostly suppressed at all wavelengths suggesting very strong packing among **1i** chromophores (Figure 9). Interestingly, application of a mechanical stress produced a partial but effective disruption of **1i** aggregates thus restoring the typical green emission of the film coming from isolated not interacting dyes (500-550 nm). Their molecular dispersion flanked by the high luminescent response due to the **1i** optical characteristics give to the film a distinct contrast in emission between the oriented portion and the pristine sample (Figure 9, inset).

Conclusion

The efficient design of innovative dye-doped polymeric materials with smart attributes requires a detailed regulation of several parameters, among which the modulation of the chromophores optical characteristics as a function of their aggregation behaviour appears the most intriguing. In this framework, the availability of reliable and predictive computational methods was found to be very beneficial. As far as the screening is concerned, it was shown capable of predicting with good accuracy the spectral behaviour of the investigated class of chromophores, allowing us to select the best candidate among a rather large set of homologues, and to produce a polymer with smart behaviour, with obvious benefits in terms of costs and time. From a computational point of view, the present study demonstrates also that experimental effects (*e.g.* solvation) are well reproduced by simulations, underlying the ability of such an approach to dissect the role of several, concomitant effects in tuning optical properties. Considering the whole spectral shape, the best choice is the adoption of vibronic models that allow for a more confident description of absorption and emission spectra line-shapes providing, at the same time, improvements with respect to the purely electronic picture in describing correctly the broadening of the electronic transitions. The latter aspect is very important in studying chromophores and in predicting their spectral behavior, this fact being directly responsible for the final color perceived by the human eye.

Once the best dye candidate was selected through the screening protocol, and effectively synthesized, a "smart" material was created by assembling the chromophore with a polymeric matrix. In fact, the selected dye when dispersed into linear low density polyethylene showed emission features depending on dye aggregation extent, *i.e.* a remarkable quenching of luminescence occurs at the highest concentration. Once a mechanical stress was applied, the dye promptly restored its bright green emission thanks to the rupture of its supramolecular structure provided by polymer matrix orientation displaying distinct mechanochromic behaviour.

A further step forward in the computational screening could stand in taking into account, at a reliable level of accuracy, the interactions of the polymeric matrix with the chromophore, extending the predictions to the whole mechanochromic material. Indeed, work in this direction is in progress in our laboratory.

Acknowledgements

This work has been supported by the Fondazione Cassa di Risparmio di Pisa under "POLOPTEL" project n. 167/09.

[1] a) X. Zhang, S. Rehm, M. M. Safont-Sempere, F. Wurthner, *Nat. Chem* **2009**, *1*, 623-629; b) Y. Sagara, T. Kato, *Nat. Chem* **2009**, *1*; c) Y. Sagara, T. Kato, *Angew Chem Int Edit* **2011**, *50*, 9128-9132; d) P. Anzenbacher, F. Li, M. A. Palacios, *Angew. Chem. Int. Ed* **2012**, *51*, 2345.

[2] J.-L. Bredas, S. R. Marder, E. Reichmanis, *Chemistry of Materials* **2011**, *23*, 309-309.

[3] a) A. Pucci, R. Bizzarri, G. Ruggeri, *Soft Matter* **2011**, *7*, 3689–3700; b) A. Pucci, G. Ruggeri, *J. Mater. Chem.* **2011**, *21*, 8282-8291.

[4] a) D. A. Davis, A. Hamilton, J. L. Yang, L. D. Cremar, D. Van Gough, S. L. Potisek, M. T. Ong, P. V. Braun, T. J. Martinez, S. R. White, J. S. Moore, Sottos, N.R., *Nature* **2009**, *459*, 68–72; b) A. Beiermann, S. L. B. Kramer, J. S. Moore, S. R. White, N. R. Sottos, *ACS Macro Lett.* **2012**, *1*, 163–166.

[5] C. Weder, *J. Mater. Chem.* **2011**, *21*, 8282-8291.

[6] a) C. J. Cramer, *Essentials of Computational Chemistry*, Second ed., John Wiley & Sons Ltd, Chichester, West Sussex, England, **2004**; b) P. Kirkpatrick, *Nat Rev Drug Discov* **2005**, *4*, 959; c) M. Cifelli, L. De Gaetani, G. Prampolini, A. Tani, *The Journal of Physical Chemistry B* **2008**, *112*, 9777-9786; d) M. McCullagh, T. Prytkova, S. Tonzani, N. D. Winter, G. C. Schatz, *The Journal of Physical Chemistry B* **2008**, *112*, 10388-10398; e) L. R. Dalton, S. J. Benight, L. E. Johnson, D. B. Knorr, I. Kosilkin, B. E. Eichinger, B. H. Robinson, A. K. Y. Jen, R. M. Overney, *Chemistry of Materials* **2010**, *23*, 430-445; f) S. Difley, L.-P. Wang, S. Yeganeh, S. R. Yost, T. V. Voorhis, *Accounts of Chemical Research* **2010**, *43*, 995-1004; g) D. Beljonne, J. Cornil, L. Muccioli, C. Zannoni, J.-L. BreÃÅdas, F. Castet, *Chemistry of Materials* **2010**, *23*, 591-609; h) A. Pedone, G. Prampolini, S. Monti, V. Barone, *Phys. Chem. Chem. Phys.* **2011**, *13*; i) R. J. Macfarlane, B. Lee, M. R. Jones, N. Harris, G. C. Schatz, C. A. Mirkin, *Science* **2011**, *334*, 204-208; j) S. Fantacci, F. De Angelis, *Coordination Chemistry Reviews* **2011**, *255*, 2704-2726; k) G. C. Schatz, *The Journal of Physical Chemistry Letters* **2011**, *2*, 125-126; l) L. Zhu, Y. Yi, Y. Li, E.-G. Kim, V. Coropceanu, J.-L. Brèdas, *Journal of the American Chemical Society* **2012**, *134*, 2340-2347.

[7] V. Barone, *Computational Strategies for Spectroscopy, from Small Molecules to Nano Systems*, John Wiley & Sons, Inc. , Hoboken, New Jersey, **2011**.

[8] a) V. Barone, J. Bloino, M. Biczysko, F. Santoro, *J. Chem. Theory Comput.* **2009**, *5*, 540–554; b) J. Bloino, M. Biczysko, F. Santoro, V. Barone, *J. Chem. Theory Comput.* **2010**, *6*, 1256–1274.

[9] F. Santoro, R. Improta, A. Lami, J. Bloino, V. Barone, *The Journal of Chemical Physics* **2007**, *126*, 084509-084513.

[10] a) G. Pietraperzia, M. Pasquini, F. Mazzoni, G. Piani, M. Becucci, M. Biczysko, D. Michalski, J. Bloino, V. Barone, *J. Phys. Chem. A* **2011**, *115*, 9603−9611; b) D. Jacquemin, E. Bremond, I. Ciofini, C. Adamo, *The Journal of Physical Chemistry Letters* **2012**, *3*, 468-471.

[11] a) S. Miertus, E. Scrocco, J. Tomasi, *Chem. Phys. Lett.* **1981**, *55*, 117; b) C. J. Cramer, D. G. Truhlar, *Chem. Rev.* **1999**, *99*, 2161; c) J. Tomasi, B. Mennucci, R. Cammi, *Chem. Rev.* **2005**, *105*; d) J. Mosnacek, M. Bertoldo, C. Kosa, C. Cappelli, G. Ruggeri, I. Lukac, F. Ciardelli, *Polymer Degradation and Stability* **2007**, *92*, 849-858; e) A. Klamt, *WIREs Comput. Mol. Sci.* **2011**, *1*; f) J. Tomasi, *WIREs Comput. Mol. Sci.* **2011**, *1*.

[12] a) J. L. Rivail, D. Rinaldi, V. Dillet, *Mol. Phys.* **1996**, *89*; b) C. Cappelli, in *Continuum Solvation Models in Chemical Physics: Theory and Applications* (Eds.: B. Mennucci, R. Cammi), Wiley, Chichester, **2007**; c) B. Mennucci, C. Cappelli, C. A. Guido, R. Cammi, J. Tomasi, *J. Phys. Chem. A* **2009**, *113*; d) A. V. Marenich, C. J. Cramer, D. G. Truhlar, C. A. Guido, B. Mennucci, G. Scalmani, M. Frisch, *J. Chem. Sci.* **2011**, *2*.

[13] a) Y. H. Wang, M. Halik, C. K. Wang, S. R. Marder, Y. Luo, *J. Chem. Phys.* **2005**, *123*; b) R. Improta, V. Barone, F. Santoro, *Angew. Chem. Int. Ed. Engl.* **2007**, *46*; c) F. Avila Ferrer, R. Improta, F. Santoro, V. Barone, *Phys. Chem. Chem.Phys* **2011**, *13*.

[14] X. Zhan, M. Yang, G. Xu, X. Liu, P. Ye, *Macromol. Rapid Commun.* **2001**, *22*, 358-362.

[15] J. Fortage, J. Boixel, E. Blart, A. Hammarström, H. C. Becker, F. Odobel, *Chem. Eur. J.* **2008**, *14*.

[16] A. Soheili, J. Albaneze.Walker, J. A. Murry, P. G. Dormer, D. L. Hughes, *Org. Lett* **2003**, *5*.

[17] F. Bellina, M. Lessi, *Synlett* **2012**, *23*.

[18] a) N. Tirelli, S. Amabile, C. Cellai, A. Pucci, L. Regoli, G. Ruggeri, F. Ciardelli, *Macromolecules* **2001**, *34*; b) A. Pucci, C. Cappelli, S. Bronco, G. Ruggeri, *J. Phys. Chem. B* **2006**, *110*.

[19] F. Donati, A. Pucci, C. Cappelli, B. Mennucci, G. Ruggeri, *J. Phys. Chem. B* **2008**, *112*.

…

Received: ((will be filled in by the editorial staff))
Revised: ((will be filled in by the editorial staff))
Published online: ((will be filled in by the editorial staff))

Entry for the Table of Contents

Smart Designing

G. Prampolini, F. Bellina, M. Biczysko, C. Cappelli, L. Carta, M. Lessi, A. Pucci, G. Ruggeri, V. Barone*

***In Silico* Designed Novel Mechanoresponsive Materials**

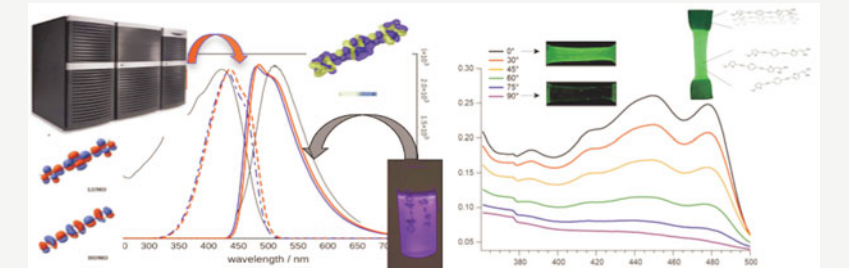

The best dye candidates, spotted by state-of-the-art quantum mechanical calculations are effectively synthesized and introduced into a polyethylene matrix, thus achieving a " *in silico* designed" mechanoresponsive "smart" material.

Besides this material can find application itself, the integration of computational and experimental techniques here reported defines an efficient protocol that can be applied to make when a selection among very similar dye candidates is required, with benefits of costs and time.